FLAW IDENTIFICATION USING ACOUSTIC EMISSION

B. WOODWARD, N.R. McDONALD

Engineering Research Division,
AAEC Research Establishment, Sutherland 2232, N.S.W., Australia

SUMMARY

Acoustic emission "signatures" contain information about the fine structure of metallurgical "source events" and their interpretation may provide a means of assessing the severity of internal flaws as well as surface flaws. The ultimate aim of this research on signature analysis is to develop a real time non-destructive testing technique having the capability of flaw "recognition" as well as flaw location in nuclear reactor components and structures under stress. Thus the requisite, unlike that in most acoustic emission work to date, is for a technique which affords discrimination between acoustic emission from different types of flaws propagating simultaneously. The approach described here requires detailed analysis of the emission signatures in terms of a specific statistical parameter, energy spectral density.

In the acoustic emission monitoring and recording system the observed energy spectrum for the waveform of a single emission "burst" is the result of a chain of modification of the frequency content of the original source event imposed by the frequency responses of the testpiece, sensor, and electronic equipment. The principle of the analysis procedure is that if all the intermediate responses in this chain remain constant then any differences in observed spectra should indicate different types of source event. Thus the method applies for groups of bursts which occur during small changes of strain, so that the testpiece geometry, and hence its spectral characteristics, remains unchanged.

In order to realise the full inspection potential of acoustic emission monitoring, data obtained from zirconium and steel testpieces have been correlated with metallurgical condition and mechanical behaviour, since the nature of emission signatures is strongly affected by the physical characteristics and internal structure of the material. During experiments, signals were tape recorded and the surface of each testpiece was recorded on movie film or videotape so that acoustic and visual information could be correlated. Large numbers of tape-recorded bursts have been analysed with a real time spectrum analyser, and statistical parameters (such as mean energy density, mean frequency and variance) derived from the spectra were calculated by an IBM 360/50 computer and selectively displayed on a line plotter. In the case of zirconium, observed differences in these parameters were an indication that the emission signals were generated by three different metallurgical mechanisms. A movie film of testpiece surface deformation revealed the occurrence of twin initiation, twin broadening and slip. Fracture events either in the zirconium matrix or in second phase particles are also possible although not obserbed directly. A direct correlation was confirmed between twin initiations and emission signals. Work is proceeding on establishing a different correlation between emission signals and stress corrosion cracks.

1. Introduction

In the field of acoustic emission, advances in technology have far outstripped advances in fundamental understanding of the phenomenon in terms of the information content of the observed signals. Thus, while sophisticated systems for locating flaw sources have received considerable attention in the literature, there appear to be no conclusive results which relate to acoustic identification of these flaws and an assessment of their severity, e.g. size, rate of propagation, degree of criticality, etc.

The importance of acoustic identification is its potential for assessing internal flaws as well as readily observable surface flaws, without the need to scan an entire structure under test as in the more traditional ultrasonic and radiographic techniques for nondestructive testing. Since acoustic emission signals are likely to contain much information about the fine structure of flaw sources, the analysis of this information is of widespread interest. In the present study, the aim is to characterise different types of flaws in terms of specific random signal parameters, the amplitude spectrum and the energy spectrum.

A number of authors have previously suggested spectral analysis as a means of categorising emission signals, notably Stephens and Pollock [1] who, although able only to demonstrate its feasibility semiquantitatively, were among the first to recognise its importance. This type of analysis has been attempted by several workers [2 - 9].

Since 1970, spectral analysis of acoustic emission signals has been used increasingly in nuclear reactor applications, primarily in pressure vessel testing programs. This has been motivated by a need to monitor emission under operating conditions. Ultimately, the objective of this type of work is to identify, in the presence of inherent reactor noise from circulating pumps and heat exchangers, not only the sources of emission but also the types of flaws that are propagating and determine whether or not these are of critical size. Several writers have contributed to this type of signal categorisation [10 - 16]. This area of research offers probably the biggest challenge to the development of flaw identification by acoustic emission signal analysis.

2. Experimental Rationale

Acoustic emission is the name given to the elastic waves generated when a solid material is deformed, cracked or undergoes a phase change. It is a dynamic phenomenon in which mechanical energy is released by metallurgical source mechanisms such as twin formation, dislocation motion, crack propagation, martensitic transformation, etc. In some materials, notably tin and wood, the mechanical activity is clearly audible; in most materials, however, these waves have small amplitudes and contain very high frequencies which cannot be detected by ear. Observed signals are usually in the form of complex decaying fast transients, or bursts, since they result from the impulse response of a vibrating system (comprised of material and detecting transducer) which behaves as a damped oscillator. The appearance of a typical burst, which has been time-expanded sufficiently for the waveform to be resolved, is shown in Figure 1.

Because acoustic emission is a random phenomenon, these signals cannot be described by explicit mathematical formulae and are therefore non-deterministic. Since their statistical properties can vary significantly from one sample to another during any stressing regime, they are also non-stationary. However, they can still be characterised by their statistical properties and, as pointed out by Papoulis [17] and Priestley [18], transient signals may be

analysed by a theory similar to that for stationary random signals. The basis of the theory is that transient signals have finite energy, and consequently a non-zero value for the mean square $\overline{x^2(t)}$, because

$$\infty > \int_{-\infty}^{\infty} x^2(t) > 0 \qquad (1)$$

For a transient signal of duration λ, the total energy of the signal may be expressed by

$$\int_0^{\lambda} E_{xx}(f)\, df = \int_0^{\lambda} x^2(t)\, dt \qquad (2)$$

$$= \lambda . \overline{x^2(t)} \qquad (3)$$

where $E_{xx}(f)$ is the energy spectral density function and the 'bar' indicates the mean square for a time λ.

With conventional monitoring and recording equipment, the observed energy spectrum (or 'output' spectrum) for a discrete acoustic emission burst is the result of progressive modificaton of the energy spectrum for an original source event (the 'input' spectrum) by a series of single input/single output (SISO) systems. Similarly the observed waveform, or signature, is the result of modification by various system impulse responses. Thus in Figure 2, the energy spectrum $E_{11}(f)$ is observed as $E_{77}(f)$, which is quite different in form and probably in bandwidth depending on the frequency response of the equipment.

In principle, knowing the responses $H_{21}(f)$, $H_{32}(f)$, etc., it is possible to derive the spectrum for each source event and then any important differences between the spectra might be interpreted in terms of different source mechanisms. Because it is very difficult to measure experimentally the total spectral response of a testpiece, the principle applied here is to assume that all the intermediate responses in the chain of modification remain constant, so that different source mechanisms are indicated directly by differences in output spectra. Equipment available for this research has enabled measurements to be made in terms of the amplitude spectral density function $A_{xx}(f)$, in which each ordinate is the square root of the corresponding ordinate in the energy spectrum. In Figure 3, however, both the amplitude and energy spectral functions are given.

For this analysis, only groups or bursts which occur during small changes of strain are considered, so that the testpiece geometry, and hence its spectral response, remains the same throughout. It has been argued by Egle and Tatro [19], and Hutton [20], that acoustic emission events give rise to longitudinal, shear, flexural and Rayleigh waves, and perhaps to other types of wave. In general, each of these wave types would excite the transducer into a different mechanical response, but for a transducer predominantly sensitive to shear waves and the shear component of flexural waves (as used here), it may be assumed that its response is the same for all source events. For the frequency range of interest (75 kHz - 300 kHz) the transducer used could 'see' any testpiece mode because with a diameter of about 2 cm it could not be situated precisely on any displacement node; thus no attenuation for particular modes was expected on account of transducer size or position. The fact that the attenuation depends on the distance between source and detector is not significant because of the small distances involved.

A review by Mahajan and Williams [21], indicates that measurements of the precise

durations of source events generated by different discrete mechanisms have never been satisfactorily established, although the durations and consequently the bandwidths of the corresponding amplitude or energy spectra are probably the keys to flaw identity. This is simply because bandwidth is inversely proportional to duration; thus two mechanisms having durations t_1 and t_2 may be identified from their spectra because these extend to frequencies $1/t_1$ and $1/t_2$ respectively. In Appendix I, it is shown how the amplitude spectrum for a single event may be characterised by a median value of frequency rather than an upper limiting frequency, a parameter more appropriate here because of the comparatively narrow bandwidth of the instrumentation used.

3. Measurement Techniques

This paper describes only techniques involving the characterisation of acoustic emission signals in terms of random signal parameters. A full description of all the interdisciplinary aspects of the research program is not included, but a flow chart showing the complete instrumentation and data interpretation system is shown in Figure 4. With two information channels, visual and acoustic, surface deformation events may be observed and the mechanisms identified, while the acoustic emission signals which these events generate may be spectrally analysed and the two sets of information correlated. In addition, emission count rates (the number of waveform 'crossovers' per second) and cumulative count (the summation of count rate over a given stressing regime) may be obtained for direct comparison with stress-strain or load-time curves.

A number of materials have been monitored for emission including mild steel, stainless steel and aluminium, but reactor-grade zirconium was chosen for most of the random signal analyses in the program because it deforms by several mechanisms at room temperature (e.g. twinning, slip and cracking), thus allowing comparison to be made of the spectra and other statistical properties of individual bursts.

Testpieces having a 'dogbone' configuration (to localise the stress concentration) and overall dimensions 10 cm long, 2.5 wide and 0.07 cm thick are loaded by a Hounsfield tensometer which is operated at constant crosshead speeds. Surface deformation events, readily observed by optical microscopy, are recorded on movie film or videotape by a 3 MHz SONY TV system. Signals from these events are detected by a sheer wave piezoelectric transducer with a response peaking at 150 kHz, filtered to remove extraneous low-frequency noise, amplified by 50-80 dB, and recorded on one channel of a high fidelity Ampex FR1300 tape recorder. The pass-band of the system is approximately 75 kHz to 300 kHz for recordings made at 152.4 cm s^{-1}. Amplitude spectral density functions are obtained from a Spectral Dynamics SD301B Real Time (Spectrum) Analyser in conjunction with an SD302A Ensemble Averager which automatically samples and averages any binary number of spectra up to 1024 (2^{10}). Each ensemble-averaged spectrum is plotted by a Philips PM8120 X-Y Recorder.

Typical burst emissions from zirconium are in the range 1 ms to 10 ms which is too short to allow sufficient sampling time for reasonable statistics; moreover, the frequency content of the signals extends well above the bandwidth of the analysis equipment, which ranges up to 20 kHz. The signals are therefore time-expanded before analysis, typically by a factor of 4096 (2^{12}), by re-recording with an auxiliary tape recorder operating at a different speed. This allows approximately eight ensembles to be averaged, depending on the duration of the burst being analysed. A time-expansion factor of 1024 (2^{10}) has also been used to improve data processing time; this allows up to ten ensembles to be

averaged but at the expense of frequency resolution.

The Spectrum Analyser is interfaced with a PDP11 computer which is programmed in the FOCAL language to calculate random signal parameters from the amplitude values stored in 500 synthesised filter locations in the analyser's memory. With this procedure, the parameters are calculated for one burst at a time under teletype control. When analysing a large number of burst signals, the amplitude values are temporarily stored in the 8K core of the PDP11 then directly transferred to disk storage via a DATAWAY link for input to an IBM360/50 computer. The data can then be processed much more quickly with a FORTRAN program. Plots of amplitude spectral density, energy spectral density, energy difference spectral density (the difference between pairs of spectra), distribution of median frequencies, and emission event histograms can be generated by this program on a CALCOMP plotter. The basic computational sequence is described in Appendix 1.

4. Results

In the earlier experiments of this research project, un-notched mild steel testpieces were used. Although mild steel was not suitable for studying different source mechanisms at room temperature, it nevertheless was useful for providing signals for development of the analysis procedure. During these experiments, a few emission bursts were found to have spectra quite different from the rest. The extent of this difference is illustrated in Figure 3 for two bursts which occurred consecutively during elastic deformation of an annealed mild steel testpiece. The bursts are considered to have derived from two different source mechanisms but no attempt was made to identify them. For most bursts, the observed spectra were very similar to the one for 'Source Mechanism A' (Figure 3), the only differences being the relative heights of the spectral peaks. The spectrum for 'Source Mechanism B', however, differs greatly in form, although such 'macroscopic' differences appeared to be unusual for both mild steel and zirconium. Usual differences between one spectrum and another were in their fine structure. Apart from those with differences only in the relative amplitudes of the spectral peaks, there were other spectra of the same general form, but peaks present in one spectrum were absent from another.

In Appendix 1, it is shown how an ensemble-averaged spectrum may be characterised by median frequency and mean amplitude or energy spectral density. The median frequencies of the two spectra shown in Figure 3 are $\bar{f}_A$ = 160 kHz and $\bar{f}_B$ = 217 kHz, although as explained earlier the spectra for most bursts were generally very similar in form, so that their median frequencies were distributed over a much narrower range than this. Representation of a large number of spectra on a single plot of mean amplitude spectral density versus median frequency is shown in Figure 5 for source events in zirconium of 3 mm grain size for a testpiece elongation from 1.0 mm to 1.5 mm (an increase of less than 0.5%). The range of mean amplitude spectral density was from 0.025 to 0.959 mV Hz^{-1} (before signal amplification).

In an ideal case, two separate source mechanisms could be identified directly if all points occurred at two frequencies only; however, Figure 5 shows a statistical spread of median frequencies ranging from 134.5 kHz to 163.7 kHz. One way of rationalising this data is shown in Figure 6 which is a plot of the number of bursts whose median frequencies over this range are in spectral windows having 1 kHz bandwidths. All the points fall into two groups. Two separate Gaussian distributions would be expected for Figure 6 if two mechanisms were active, but there is some departure from this ideal. The figure also shows that relative durations for two such mechanisms may be obtained, because the higher the median of

the distribution the shorter is the duration.

Since most of the observed surface deformation was by twin initiation, it is likely that this mechanism accounts for most of the large distribution, with a most probable median frequency spectral window of 147-148 kHz. However, in Figure 7, showing data for the two separate elongation increments 1.00 to 1.25 mm and 1.25 to 1.50 mm, two overlapping distributions between 143 kHz and 159 kHz are evident as well as a third distribution between 135 kHz and 142 kHz (which has too few events to be considered separated into smaller distributions as suggested by Figure 7). Thus three different mechanisms are indicated. In addition to twin initiation a definite degree of twin broadening and a small amount of slip took place which may account for the two other distributions. Fracture events in either the zirconium matrix or in second phase particles were also possible although not observed directly.

These results have demonstrated that differences between various source events may be observed using statistical descriptive parameters if a large enough number of events are considered (in the experiment illustrated by Figures 5, 6 and 7 there were 345 events. By using broader bandwidth instrumentation, differences in observed spectra should be more pronounced and fewer events may be required to show spectral characteristics for the different mechanisms.

5. Conclusions

Random signal techniques have been applied to the problem of identifying different metallurgical source mechanisms which are initiated by loading testpieces of various materials, particularly zirconium. It has been found that marked differences can occur in the fine structure of the amplitude or energy spectra of individual acoustic emission burst waveforms. There was also some evidence of different bursts having spectra so different that their predominant frequencies were widely separated. These differences, although difficult to quantify, are considered to be indicative of different metallurgical source mechanisms. Spectral analysis of acoustic emission bursts from the zirconium testpieces used here have pointed to three mechanisms. Direct observation showed that while the predominant mechanism was twin initiation, there was also some twin broadening and slip. Fracture events in the zirconium matrix or in second phase particles were also possible mechanisms, although they were not observed directly.

The main limitation in identifying source mechanisms by their amplitude or energy spectra lay in the use of a comparatively narrow bandwidth (300 kHz). Observations indicated that, because source event durations were so short and the corresponding energy spectra so extensive in bandwidth, more information would be obtained if studies were extended to, say, 3 MHz. Any differences in the spectra of source events would then be more easily identified because it is at the higher frequencies that the spectra for source events of differing durations should be most easily resolved. This should lead to better identification of metallurgical source mechanisms in terms of the random statistical properties of acoustic emission signals, and opens up the possibility for acoustically assessing the severity of propagating internal flaws in structures or components as well as readily observable surface flaws.

6. Acknowledgements

The authors thank Dr. T.J. Ledwidge and Dr. R.W. Harris for many helpful discussions, Messrs. B.R.A. Wood and M.J. Hincksman for carrying out the majority of the experimental work, and Dr. G.W. Cox and Mrs. J.I. Faulkner for advice and assistance with computing.

References

[1] STEPHENS, R.W.B. and POLLOCK, A.A. 'Waveforms and Frequency Spectra of Acoustic Emissions', J. Acoust. Soc. Am., 50, 904-910, 1971.

[2] ONO, K., STERN, R. and LONG, Jr, M. Acoustic Emission (ASTM Special Technical Publication 505, Philadelphia), 152-163, 1971. 'Application of Correlation Analysis to Acoustic Emission'.

[3] NAKASA, H. 'Application of Acoustic Emission Techniques to Material Diagnostics', Proc. Symp. Nuclear Power Plant Control and Instrumentation, Prague, IAEA-SM-168/D-5, 462-478, 1973.

[4] GREEN, A.T. 'Stress Wave Emission and Fracture of Prestressed Concrete Reactor Vessel Materials', Technical Report DRC-71-3 (Dunegan Research Corporation), 1971.

[5] FINKEL, V.M. and SEREBRYAKOV, S.V. 'Radiation of Sonic and Ultrasonic Waves during Growth of Cracks in Steel', Phys. Metals Metallogr., 25, 169-175, 1968.

[6] GREEN, A.T., LOCKMAN, C.S. and STEELE, R.K. 'Acoustic Verification of Structural Integrity of Polaris Chambers', Modern Plastics, 41, 137-139, 1964.

[7] MEHAN, R.L. and MULLIN, J.V. 'Analysis of Composite Failure Mechanisms using Acoustic Emission', J. Comp. Mater., 5, 266-269, 1971.

[8] CURTIS, G.J. 'Acoustic Emission in Stressed Epoxy Bonded Structures', UKAEA Report AERE-R7684, 1974.

[9] SCHOFIELD, B.H. Acoustic Emission (ASTM Special Technical Publication 505, Philadelphia), 11-19, 1971. 'Research on the Sources and Characteristics of Acoustic Emission'.

[10] PARRY, D.L. and ROBINSON, D.L. 'Incipient Failure Detection by Acoustic Emission - A development and Status Report', Report IN 1398, 10-87, 1970.

[11] EISENBLATTER, J. 'Acoustic Emission Analysis as a Non-Destructive Test Method for Monitoring Reactor Pressure Vessels', 1st Int. Conf. on Structural Mechanics in Reactor Technology, Berlin, 1971.

[12] CHRETIEN, N. and TOMACHEVSKY, E. 'Application de l'Emission Acoustique an Centre d'Etudes Nuclaires de Saclay', Technical Report IAEA-145, 1972.

[13] VETRANO, J.B. and JOLLY, W.D. 'In Service Acoustic Emission Monitoring of Reactor Pressure Vessels', Mat. Eval., 30, 9-12, 1972.

[14] BRET, A., GAILLARD, M. and LECHEL, V. 'Detections des Emissions Acoustiques dans le Reacteur Rapsodie', Proc. Int. Conf. on Engineering of Fast Reactors for Safe and Reliable Operation, Karlsruhe, 1, 434-453, 1972.

[15] GASC, B. and TOMACHEVSKY, E.G. 'Surveillance des Reacteurs par les Methodes de Detections d'Emission d'Ondes de Constrainte et de Detection Acoustique', Proc. Symp. on Nuclear Power Plant Control and Instrumentation, Prague, IAEA-SM-168/D-6, 479-494, 1973.

[16] BUCK, J.S. and GRAHAM, L.J. 'Acoustic Emission Testing Experience at the EBOR Facility', Addendum Report, EEI Project RP 79 - A Joint Industry/Utility Program to Develop NDT Techniques for Nuclear Reactor Inspection, 15-38, 1973.

[17] PAPOULIS, A. The Fourier Integral and its Applications, (McGraw-Hill, New York), 1962.

[18] PRIESTLEY, M.B. 'Time-Dependent Spectral Analysis and its Application in Prediction and Control', J. Sound Vib., 17, 517-534, 1971.

[19] EGLE, D.M. and TATRO, C.A. 'Analysis of Acoustic-Emission Strain Waves', J. Acoust. Soc. Am., 41, 321-327, 1967.

[20] HUTTON, P.H. 'Acoustic Emission Monitoring for Continuous Crack Detection in Nuclear Reactor Pressure Boundaries', Report BNWL-1597, 1971.

[21] MAHAJAN, S. and WILLIAMS, D.F. 'Deformation Twinning in Metals and Alloys', Int. Met. Rev., 18, 43-61, 1973.

APPENDIX I

COMPUTED RANDOM SIGNAL PARAMETERS

Once the output amplitude spectral density (here $A_{77}(f)$ corresponding to $E_{77}(f)$ in Figure 2) for an acoustic emission signal is obtained experimentally, other random signal parameters may be derived directly. The computational sequence for each ensemble-averaged amplitude spectrum using the FORTRAN program is as follows:

(i) 500 values of frequency are read in, where f_1 = 0.1 Hz and f_{500} = 99.9 Hz. The resolution, or bandwidth, of each spectrum is therefore 0.2 Hz and the frequency range is appropriate for signals time-expanded by a factor of 2^{12}.

(ii) 500 values of amplitude spectral density in V Hz^{-1} are read in.

(iii) The area under the amplitude spectrum is calculated by numerical integration using the trapezoidal rule. The frequency, which divides this area exactly by two, gives the median frequency $\bar{f}$.

(iv) The 500 amplitude values are summed and divided by 500 to give the mean amplitude spectral density $\overline{A_{77}^{T}(f)}$. Thus $\bar{f}$ and $\overline{A_{77}^{T}(f)}$ essentially reduce the complete amplitude spectrum to a single point, which is the centroid of the area under the spectrum. Figure 5 shows a large number of such points.

(v) The number of centroids per 1 kHz bandwidth is calculated and a histogram is plotted to resolve any different types of spectra present. Figures 6 and 7 are examples.

(vi) By squaring each of the 500 amplitude values the energy spectrum $E_{77}(f)$ is obtained and its mean value $\overline{E_{77}(f)}$ may be calculated as (iv).

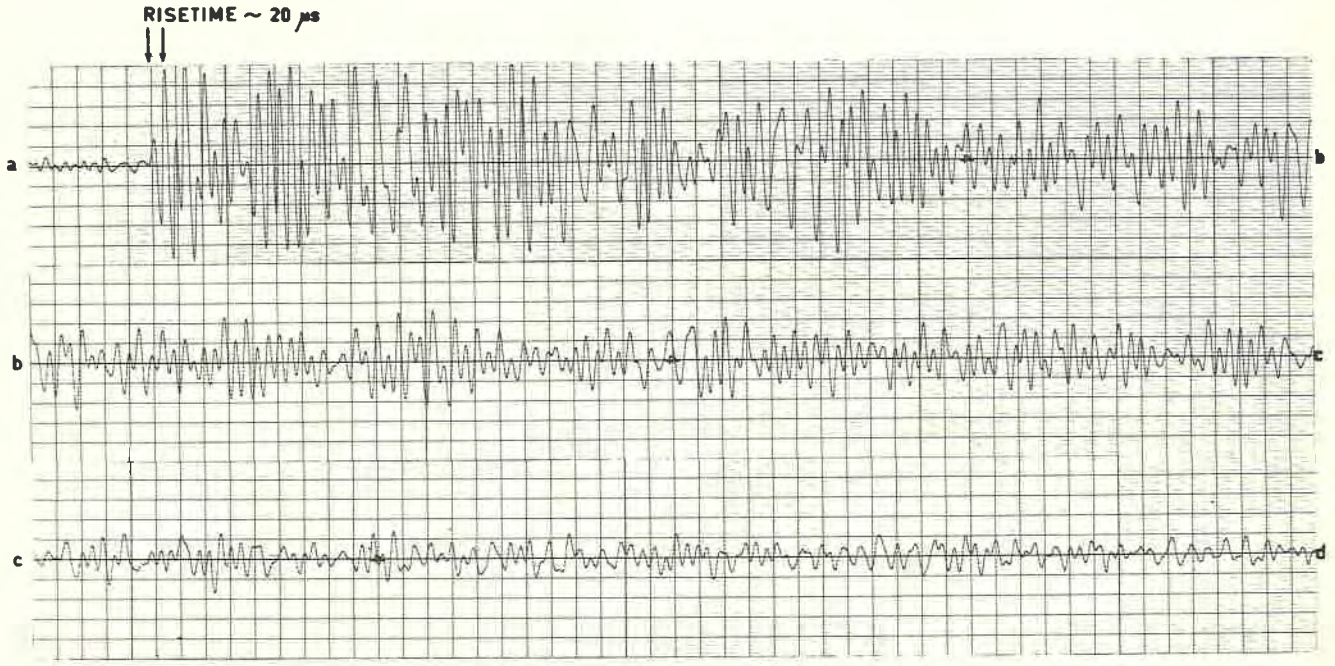

FIG. 1 RESOLVED WAVEFORM OF ONE BURST TIME-EXPANDED × 32,768 (2^{15})
TIMESCALE : 6 μs mm^{-1} on chart.
AMPLITUDE SCALE: 50mV mm^{-1} after 80dB signal gain.

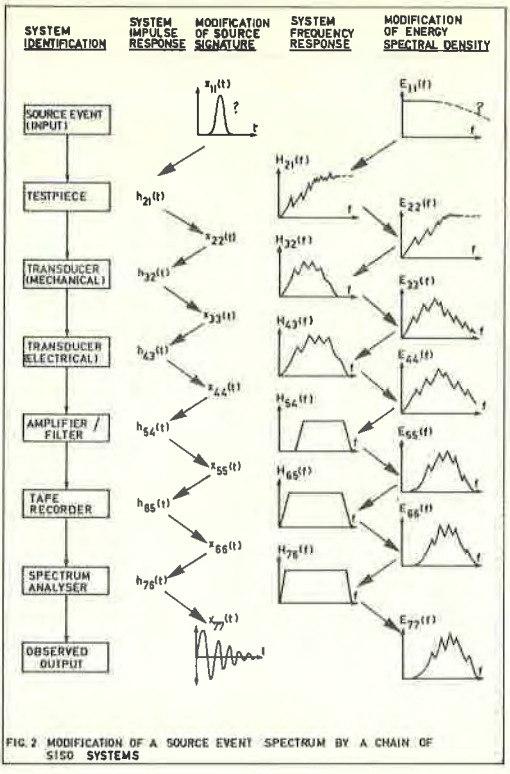

FIG. 2 MODIFICATION OF A SOURCE EVENT SPECTRUM BY A CHAIN OF SISO SYSTEMS

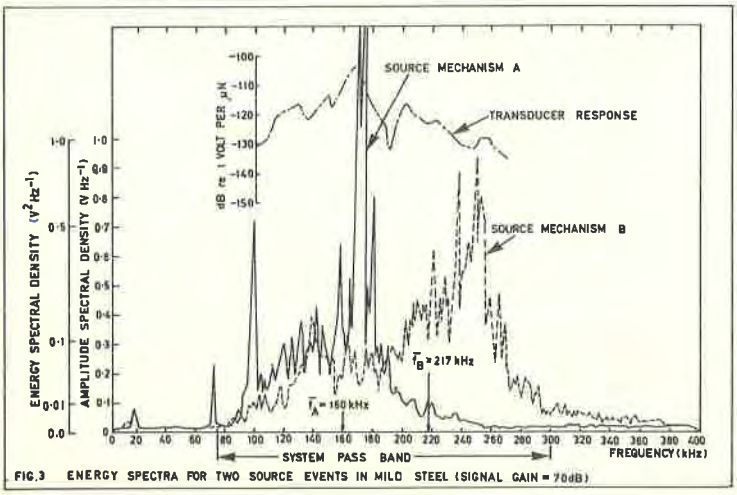

FIG.3 ENERGY SPECTRA FOR TWO SOURCE EVENTS IN MILD STEEL (SIGNAL GAIN = 70dB)

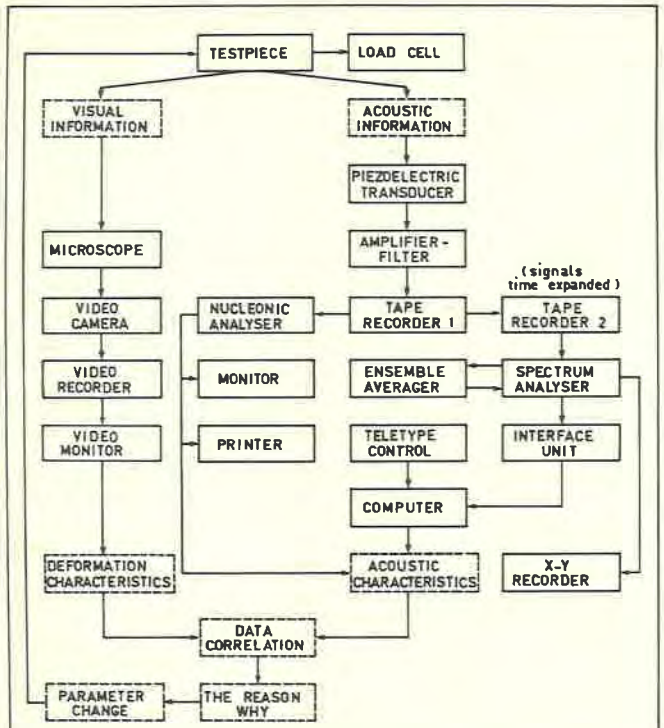

FIG. 4 INSTRUMENTATION AND DATA INTERPRETATION SYSTEM.

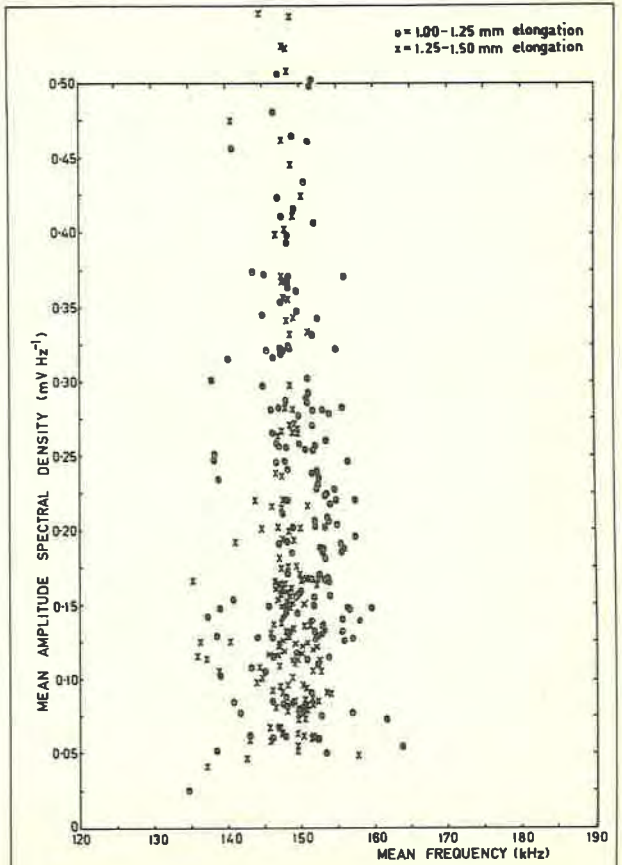

FIG. 5 DISTRIBUTION OF SPECTRA FOR A.E. BURSTS FROM ZIRCONIUM (3mm GRAIN SIZE)

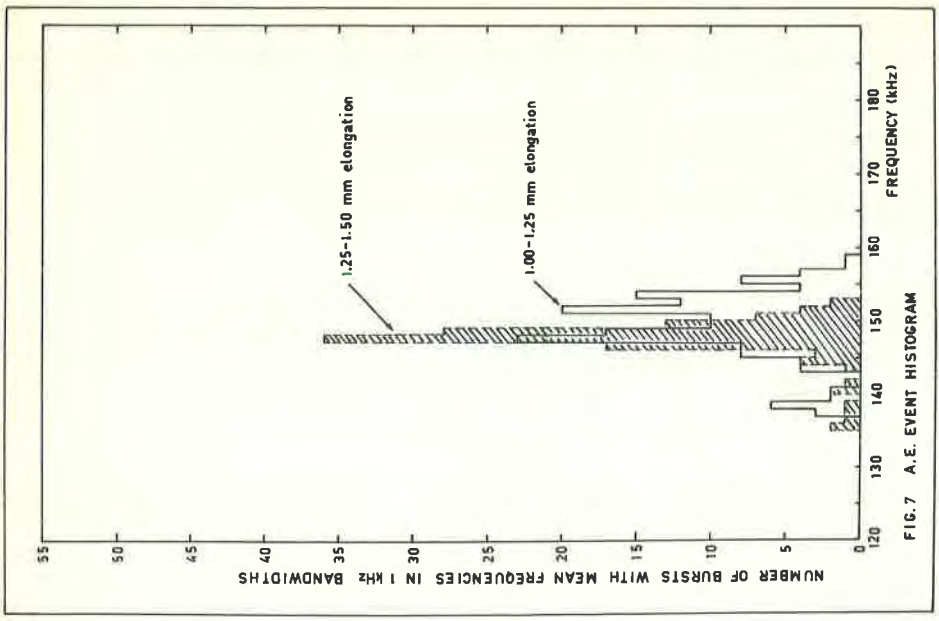

FIG.7 A.E. EVENT HISTOGRAM

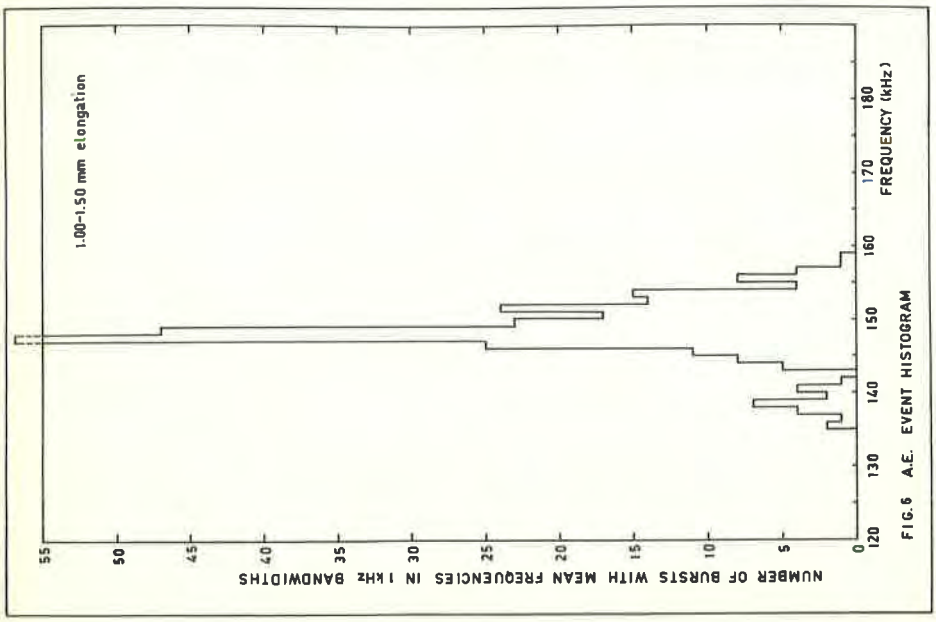

FIG.6 A.E. EVENT HISTOGRAM